Hindawi
Shock and Vibration
Volume 2019, Article ID 1903752, 9 pages
https://doi.org/10.1155/2019/1903752

Research Article

Experimental Study on Track-Bridge Interactions for Direct Fixation Track on Long-Span Railway Bridge

Jung-Youl Choi,[1] Jee-Seung Chung,[2] and Sun-Hee Kim[3]

[1]*Assistant Professor, Department of Railroad Construction & Safety Engineering, Dongyang University, No. 145 Dongyangdae-ro, Punggi-eup, Yeongju-si, Gyeongsangbuk-do 36040, Republic of Korea*
[2]*Professor, Department of Railroad Construction & Safety Engineering, Dongyang University, No. 145 Dongyangdae-ro, Punggi-eup, Yeongju-si, Gyeongsangbuk-do 36040, Republic of Korea*
[3]*Assistant Professor, Department of Architectural Engineering, Gachon University, 1342 Seongnamdaero, Sujeong-gu, Seongnam-si, Gyeonggi-do 13120, Republic of Korea*

Correspondence should be addressed to Sun-Hee Kim; shkim6145@gachon.ac.kr

Received 15 October 2018; Revised 29 November 2018; Accepted 18 December 2018; Published 28 January 2019

Academic Editor: Giuseppe Ruta

Copyright © 2019 Jung-Youl Choi et al. This is an open access article distributed under the Creative Commons Attribution License, which permits unrestricted use, distribution, and reproduction in any medium, provided the original work is properly cited.

The rail and track girder of the direct fixation track (DFT) system on the Yeongjong Grand Bridge (YGB) in Korea exhibit integrated behavior. Therefore, unlike the DFT system in general concrete tracks, the track support stiffness (TSS) of the DFT system on the YGB cannot be evaluated with only the displacement of the rail. The actual TSS of the DFT system supported by the flexible track girders was lower than that of the DFT system supported by the general substructure. For this reason, field measurements and a finite element analysis that reflects the actual operating speed of railroad vehicles on the YGB (i.e., Airport Railroad Express (AREX), nonstop Airport Railroad Express (AREX Express), and Korea Train Express (KTX)) were conducted in this study to determine the interactions between the rail and the track girder. The results indicated that the DFT system on the YGB is supported by track girders that exhibit relatively flexible behavior. As a result, the TSS is directly influenced by the bending stiffness of the track girder.

1. Introduction

Numerous studies have been conducted on the rail support. The dynamic response to rail support was studied by researchers by performing the theoretical study and the finite element analysis (FEA) [1–6]. The dynamic response of a track is not affected by dynamic properties of the train other than its unsprung mass.

Lou et al. [3] presented a rail-bridge coupling element of unequal lengths, in which the length of a bridge element was longer than that of a rail element, to investigate the dynamic problem of train-track-bridge interaction systems.

According to the study by Dinh et al. [4], use of formulation of three-dimensional dynamic interactions between a bridge and a high-speed train using wheel-rail interfaces has been adopted.

Boindi et al. [5] presented the vibration of railway bridges under moving trains taking into account that the track structure has been checked through appropriate comparisons with the finite element approach based on the use of a bridge-track-vehicle element.

Zakeri et al. [6] presented the vertical response of railway tracks subjected to moving train by a dynamic analysis method.

In this paper, the rail support responses are investigated by performing field measurements and numerical analysis with track support stiffness of the direct fixation track on the railway bridge.

The track system on the Yeongjong Grand Bridge (YGB) is a direct fixation track (DFT) attached to a long-span special bridge (cable and truss), and its concept originated from the track style of the Great Seto Bridge in Japan [7]. Such a track type is the only special case in Korea, which leads to the lack of studies thus far [7].

As shown in Figure 1(a), the track system on the YGB is installed with a direct fixation rail fastening system on top of the track girder. Moreover, as shown in Figure 1(b), it is continuously arranged with simple beam-type track

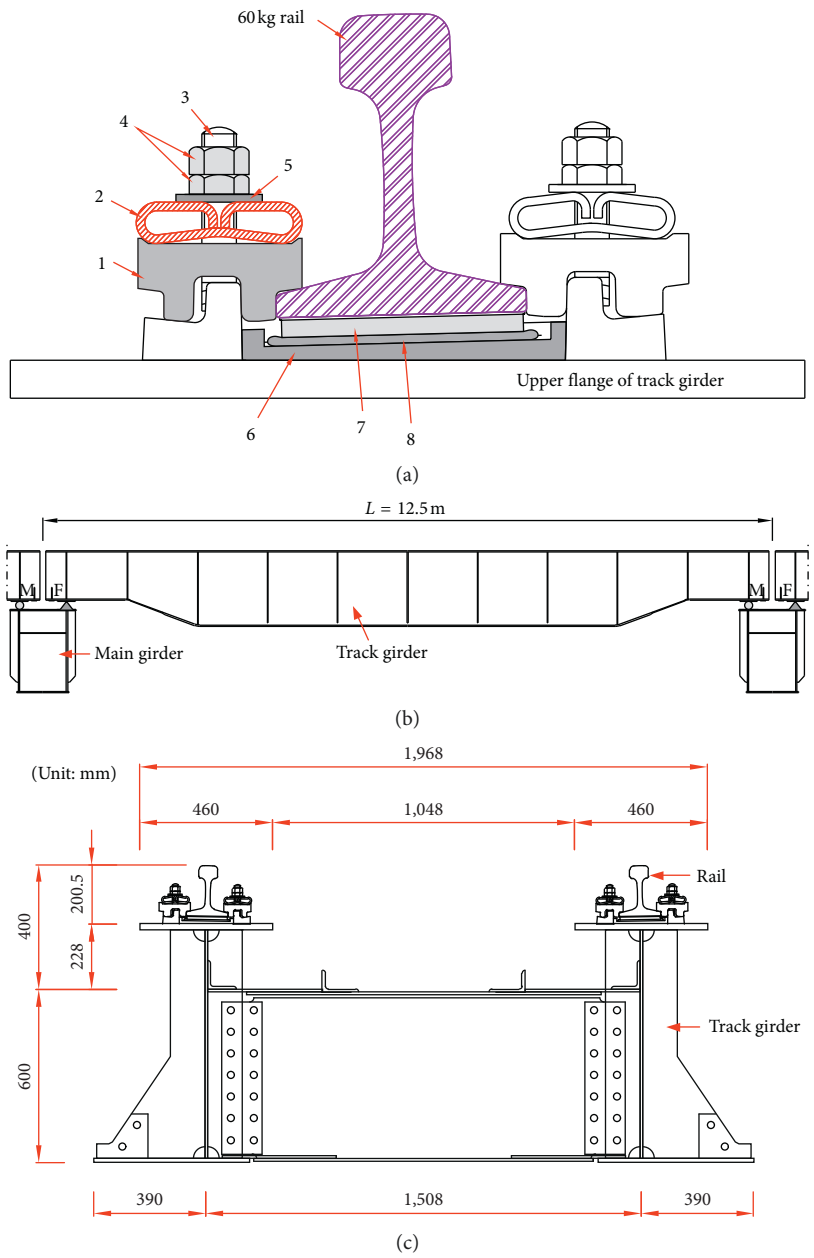

Figure 1: Schematics of the direct fixation track system. (a) Direct fixation rail fastening system: (1) insulation block; (2) leaf spring; (3) bolt; (4) antiloosening nut; (5) washer; (6) insulation plate; (7) rail pad; (8) adjustable pad. (b) Side view of the track girder. (c) Cross section of the track girder [7].

girders with a length of 12.5 m for supporting the rail. The rail applied to the YGB weighs 60 kg, and the DFT has a design speed of 110 km/h. Moreover, the direct fixation rail fastener is applied with a flat spring joint and adjusting packing as an adjustable pad and the antiloosening nut [7], as shown in Figure 1(a).

In addition, the DFT on the YGB exhibits integrated behavior because the rail and track girder are rigidly connected together by the direct fixation rail fastening system, as shown in Figure 1(c). In general, the track support stiffness (TSS) of a direct fixation applied to concrete tracks can be calculated on the basis of the deflection of the rail. However, owing to its bending behavior, the bending stiffness of the track girder must be accounted for in the calculation in order to evaluate the actual TSS of the DFT on the YGB. Therefore, by performing field measurements of the tracks and considering the operational velocity of the trains that run on the DFT of the YGB (i.e., Airport Railroad Express (AREX), nonstop Airport Railroad Express (AREX Express), and Korea Train Express (KTX)), the actual TSS of the DFT was evaluated in this study.

2. Numerical Analysis

2.1. Numerical Analysis of the Direct Fixation Track on the Yeongjong Grand Bridge. To analyze the behavioral characteristics of the DFT on the YGB, LUSAS 15.0, a finite

element analysis program, was used for the three-dimensional (3D) numerical analysis, and the results were compared with the field measurements. The major parameters for the numerical analysis of the DFT system are listed in Table 1.

In order to reflect the structural characteristics of the DFT on the YGB to the fullest, the track girder and vertical stiffener were expressed as the 3D shell elements as shown in Figure 2(a) based on the design drawing. The rail, cross beam, and bracing were modeled as beam elements, and the rail pad was modeled as a spring element through which the displacement of the rail and track girder that occurs during a moving train load was examined.

As shown in Figure 2(b), the dynamic vertical wheel load of a KTX train, which runs on the rail at a speed of 90 km/h, was modeled as a time-history function, and the moving load, which passes on the rail in predetermined intervals, was applied to the analysis to reflect the actual operational velocity of the train.

2.2. Results of the Numerical Analysis. Numerical analysis measured displacement and stiffness for rail superstructure-infrastructure direct fixation systems also in view of using for validating simulation models and procedures.

The results showed that the maximum deflection at the central part of the track girder was approximately 3.82 mm, as shown in Figure 2(c). This result had an error of less than ~5–8% in comparison with the actual vertical displacement result of a rail and track girder by field measurements (rail: 3.97 mm and track girder: 4.18 mm), indicating that the analysis model is appropriate. Moreover, the vertical deflection at each position on the track girder, as calculated by the numerical analysis, was utilized to calculate the equivalent spring of the track girder considering the stiffness of the track girder. It was found that the stiffness of the girder is influencing the value of track support stiffness.

2.3. Field Measurements

2.3.1. Test Site and Tested Vehicles. To experimentally evaluate the performance of the existing DFT on the YGB, field measurements of the operational track were conducted. The location of the measurement was selected as the DFT inside the truss bridge, as shown in Figures 3(a) and 3(b).

The vehicles operating in the measurement section are AREX (normal train), AREX Express (semi-high-speed train), and KTX (high-speed train), which have different operational velocities and wheel loads. In this study, the dynamic responses of the track, which were generated while the trains are running, were used for the analysis. The properties and photographs of the trains running in the measurement section are presented in Table 2 and Figures 3(c) and 3(d), respectively.

2.3.2. Establishing a Measurement System. In this study, the dynamic wheel load for each train type applied to the DFT on the YGB and the vertical displacements of the rail and track girder were measured. On the basis of the results, the performance of the DFT on the YGB in the in-service condition was evaluated. The dynamic wheel load for each position of the track girder including the support, the quarter, and the center of the span as well as the vertical displacement of the rail and the vertical displacement of the track girder was measured, as shown in Figure 3(e). Figures 3(f) and 3(g) show the sensors installed at the site. The vertical wheel loads were measured using a wheel load sensor, i.e., shear strain gauges coupled to a full Wheatstone bridge circuit [8]. The strain gauge bridges were calibrated using a hydraulic ram and a load cell to obtain measurements with an accuracy of 2% [8]. The shear strain gauges were attached to both rails between two consecutive rail supporting points. In order to prevent data distortion and loss, the sampling rate was set to 1 kHz [8]. The vertical rail and track girder displacements were measured using displacement transducers mounted on a jig anchored at the side bridge inspection passage, where it was not affected by the passing train, as shown in Figures 3(b)–3(g).

Table 1: Parameters for the finite element model.

Parameter	Value
Rail	
Weight	60 kg/m
Elastic modulus	210 kN/mm^2
Second moment of inertia	30,900,000 mm^4
Sectional modulus	396,000 mm^3
Track girder	
Length	12.5 m
Steel grade	SM 400
Upper flange	PL-460 × 22 × 12.402
	PL-540 × 14 × 2.036
Bottom flange	PL-300 × 25 × 8.470
	PL-200 × 10 × 1.178
Bracing	L-100 × 100 × 10 × 1.051
Cross beam	L-90 × 90 × 10 × 1.200
Web	PL-583 × 9 × 1.239
Vertical stiffener	PL-120 × 12 × 808
	PL-376 × 12 × 808
Rail fastener	
Rail supporting point spacing	0.625 m
Spring stiffness of rail pad (dynamic)	133 kN/mm

3. Results

A wheel load sensor and displacement transducer were installed on the rail and track girder in order to measure the characteristics of the dynamic wheel load, the vertical displacement of the rail, and the vertical displacement of the track girder of the direct-fixation-track-type rail while the trains were running. Sample data for the dynamic wheel load, the vertical displacement of the rail, and the track girder displacement for each train passing through the tested section are shown in Figures 4(a)–4(f).

The results shown in Figures 4(g) and 4(h) indicate that the changes in the dynamic wheel load and rail vertical displacement according to the change in the speed of each train are not very significant. Therefore, the dynamic response of the DFT is not directly influenced by the velocity of the trains if they are running within the operational velocity

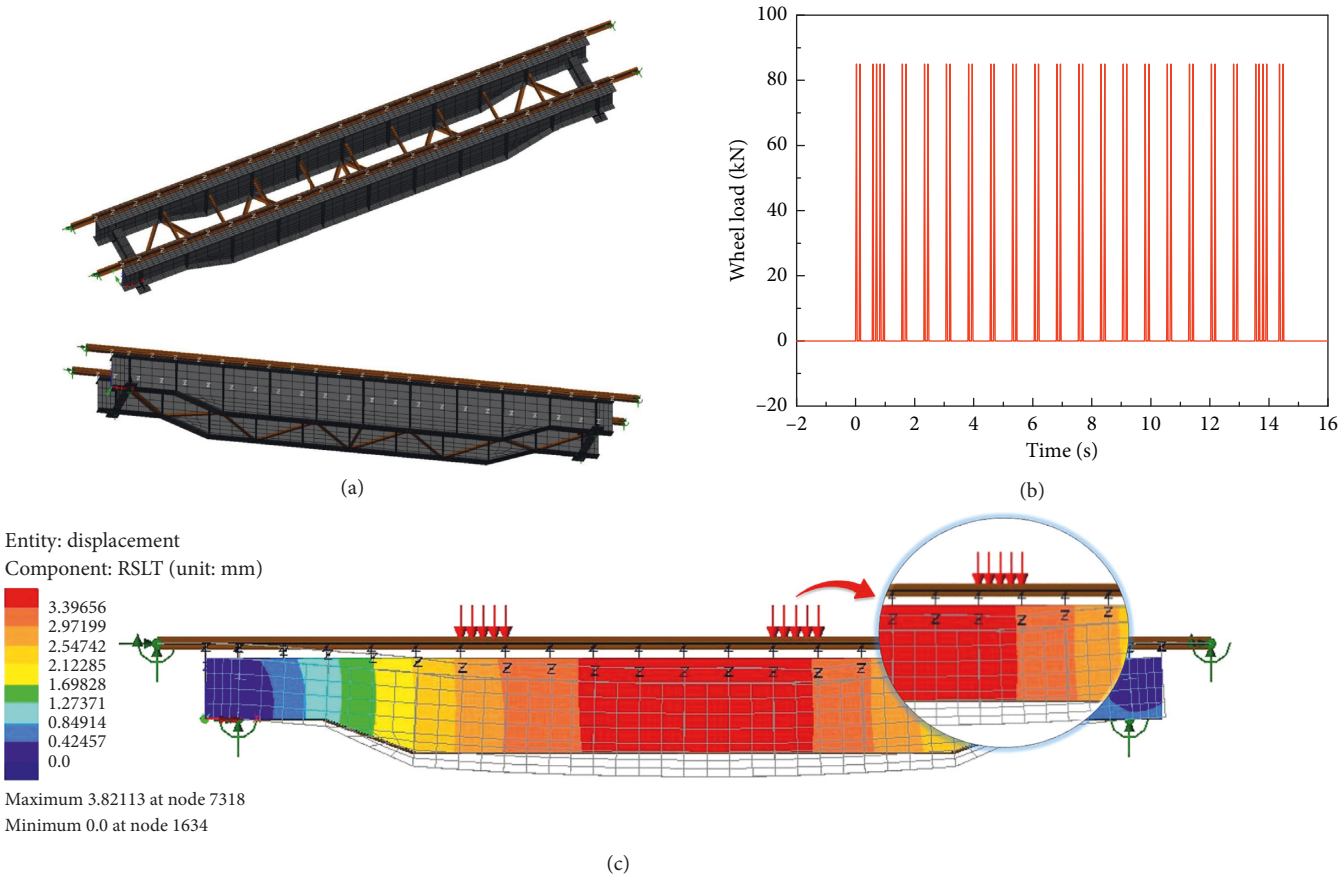

Figure 2: Finite element analysis. (a) 3D view of the FE model. (b) Example of the time-history function (KTX, 90 km/h). (c) Analysis results for the displacement of the rail and track girder.

range, as shown in Figure 4(i). Moreover, the distribution ranges of the dynamic wheel load, rail vertical displacement, and track girder displacement of AREX and AREX Express were similar, whereas the KTX train exhibited a higher dynamic wheel load, rail vertical displacement, and track girder displacement than the AREX train by approximately 54%, 46%, and 43%, respectively. This is due to the difference in the designed wheel loads between the AREX and KTX and not the dynamic amplification effect originating from the velocity.

As shown in Figures 4(h) and 4(i), the difference between the rail vertical displacement and the track girder displacement was approximately 3–6%, indicating that the flexible behaviors of the rail and track girder are very similar. This is due to a structural characteristic, where the upper flange of the track girder adopts the direct-fixation-type rail fastening system as shown in Figure 1(a). In the case of the tested track, the rail pad (k_{pad} = 133 kN/mm) is relatively hard, and a rail fastener with a strong fastening force is used. Therefore, the rail and track girder are coupled with a strong force and exhibit integrated behavior since there are no other components that provide elastic behavior between the rail and track girder.

3.1. Calculation of the Measured Track Support Stiffness. The TSS is an index for evaluating the track performance, which indicates the support performance of the track against the train load and provides information for evaluating the quality and condition of track components [1, 7, 9]. The TSS is also an important design variable for designing the track and substructures and is directly influenced by various structural characteristics and the elasticity range for each track system [1, 7, 9]. Since the magnitude of the TSS directly affects the static and dynamic displacements of a track and its overall performance, it is an important factor that directly influences the stability and safety of train operations [1, 7, 9].

Figure 5 shows a model of the DFT system considering the equivalent spring stiffness of the track girder. The TSS of the DFT, which is supported by a relatively flexible track girder, can be calculated by the combined stiffness of the series of linear spring elements with different spring stiffness placed at the rail supporting point composed of a rail pad and track girder connected in series using equation (1). Therefore, as shown in Figure 5, the stiffness at the rail supporting point of the DFT system could be determined by both the spring stiffness of the serially arranged elastic material (rail pad) and the equivalent spring stiffness of the track girder considering the bending stiffness (flexural rigidity) of the track girder [9]. These quantities were substituted into a linear spring model in order to calculate the actual rail supporting point stiffness.

Moreover, the stiffness at the rail supporting point of the DFT substituted into the linear spring model, which is the

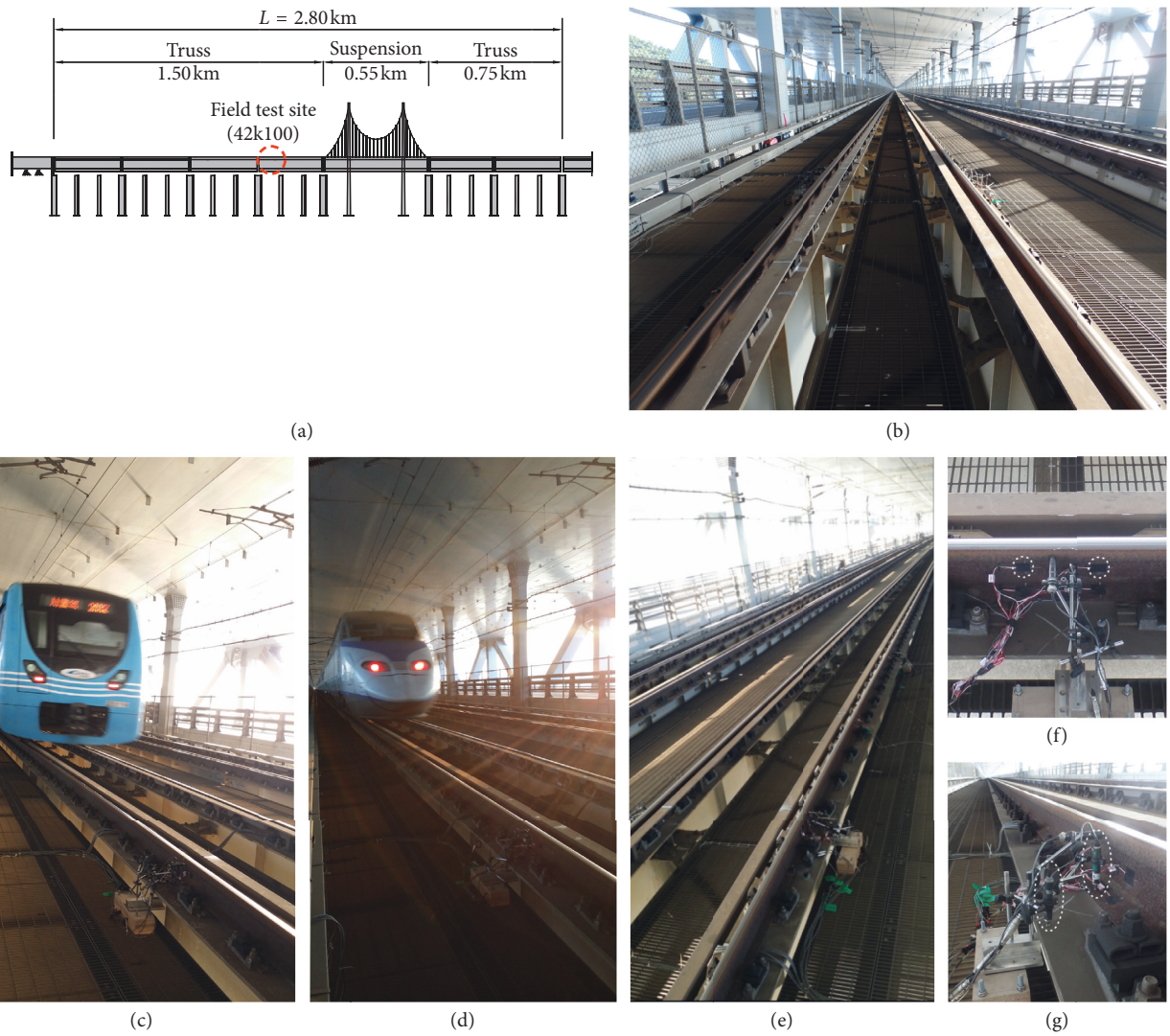

Figure 3: (a) Location of the measurement; (b–g) vertical rail and track girder displacements measured using displacement transducers mounted on a jig anchored at the side bridge inspection passage, where it was not affected by the passing train.

Table 2: Properties of the tested train.

	AREX	AREX Express	KTX
Train composition	Tc1-M-M′-T1-M′-Tc2	P-M-16R-M-P	
Total length of train (m)	120.90	120.90	388.10
Axle distance (mm)	2,200	2,200	3,000
Wheel diameter (mm)	860	860	920
Maximum speed (km/h)	120	120	330
Effective beating distance (m)	13.8	13.8	18.7
Designed wheel load (kN)	40.94	50.81	85

Note. KTX: P = power car; M = motorized trailer; R = passenger car. AREX: Tc = control car; M′ = motorized power car; T1 and T2 = passenger cars.

combined spring stiffness of the rail pad and the equivalent spring stiffness considering the bending stiffness of the track girder, is calculated as follows [7, 9]:

$$k_s = \frac{1}{\left(1/k_{\text{rail pad}}\right) + \left(1/k_{\text{track girder}}\right)}, \quad (1)$$

where k_s is the stiffness at the rail supporting point, $k_{\text{rail pad}}$ is the rail pad stiffness, and $k_{\text{track girder}}$ is the equivalent stiffness of the track girder.

The dynamic wheel load and the vertical rail and track girder displacements measured for each tested section were used to calculate the measured TSS of the DFT on the YGB.

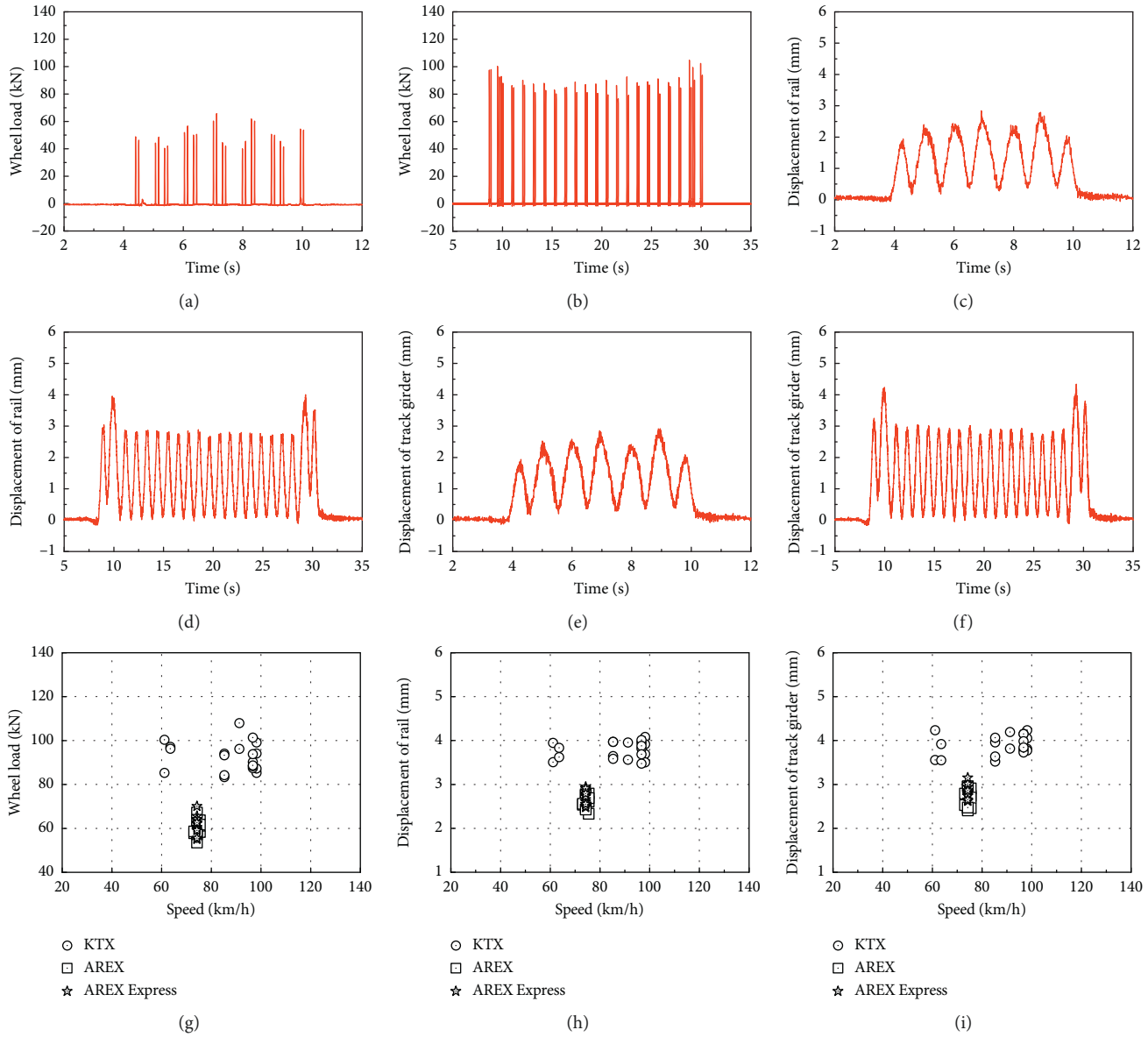

Figure 4: Examples of measured data: (a) wheel load (AREX); (b) wheel load (KTX); (c) rail displacement (AREX); (d) rail displacement (KTX); (e) track girder displacement (AREX); (f) track girder displacement (KTX). Measurement results of a direct fixation track on a bridge according to train speeds: (g) wheel load; (h) rail displacement; (i) track girder displacement.

The measured TSS is the ratio of the maximum measured wheel load to the maximum rail vertical displacement and is capable of yielding the TSS in the in-service condition [8]:

$$k = \frac{F_{\text{rail mid}}}{d_{\text{rail mid}}}, \tag{2}$$

where k is the measured TSS (kN/mm), $F_{\text{rail mid}}$ is the maximum wheel load (kN) at the center between the rail supporting points, and $d_{\text{rail mid}}$ is the maximum rail displacement (mm) at the center between the rail supporting points [8]. The wheel load, rail vertical displacement, and track girder displacement measured at the center of the track girder for each train were used to calculate the measured TSS, as shown in Figure 6.

The measured TSS according to the changes in the train speed was approximately 23 ± 5 kN/mm, as shown in Figure 6(a), indicating that the differences in the designed wheel load and train velocity do not directly influence the measured TSS. Moreover, the designed TSS calculated from the spring stiffness test results using the direct fixation rail fastening system assembly exhibited a fairly large deviation from the measured TSS. Therefore, the actual TSS of the DFT including the track girders was overestimated. Thus, the actual TSS of the DFT system should be evaluated by the TSS, which reflects the deflection of the track girder that was affected by the bending stiffness of the track girder, as demonstrated by the experiment.

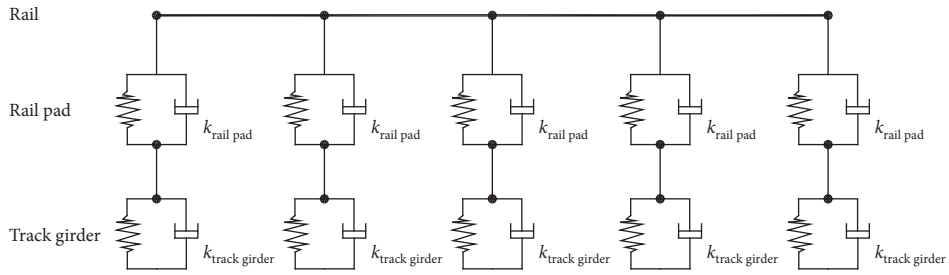

FIGURE 5: Spring stiffness model of the direct fixation track at the rail supporting points. k_{pad} = rail pad stiffness (kN/mm). $k_{\text{track girder}}$ = equivalent stiffness of the track girder (kN/mm).

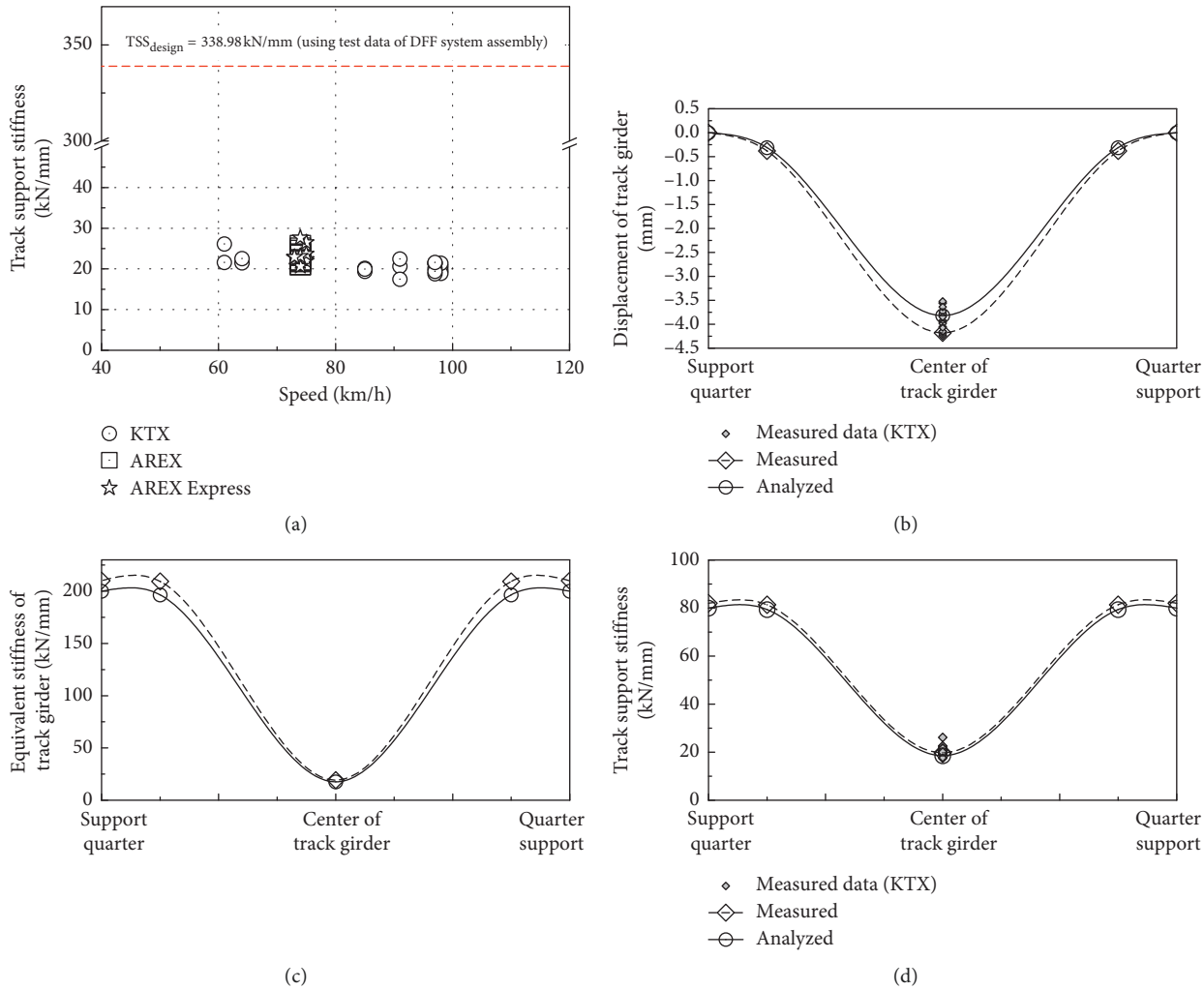

FIGURE 6: (a) Measurement results of track support stiffness for each train type. Comparison between analysis and experimental results: (b) displacement of the track girder; (c) equivalent stiffness of the track girder; (d) the track support stiffness.

3.2. Results and Analysis. The results of the analysis and measurements show that the analyzed and measured vertical displacements of the track girder in Figure 6(b) were similar, indicating that the DFT supported by track girders has a similar deflection for both the rail and track girder (Figures 4(h) and 4(i)). Therefore, the TSS of the DFT placed on top of the relatively flexible track girder is directly influenced by the bending stiffness of the track girder and the deflection that has the same position. Therefore, the analytical displacement of the track girder calculated on the basis of the numerical analysis model was compared with the measured displacement. By using the analysis and measurement results, the equivalent spring stiffness reflecting the stiffness (deflection) of the track girder was calculated.

The equivalent spring stiffness of the track girder for each position, which was calculated on the basis of the design specifications, is presented in Table 3.

Figure 6(b) shows the vertical displacement for each position on the track girder, as calculated by the numerical analysis and field measurements. On the front end of the track girder ($L/4$, quarter of the span), the analysis and measured results for the deflection were very similar. At the center of the span, the difference was less than ~5–8%, which indicates that the numerical model reflects the measurement results well.

By using the equivalent spring stiffness using the designed stiffness of the track girder (Table 3) and the measured vertical displacement of the track girder, the equivalent spring stiffness of the track girder was calculated, as shown in Figure 6(c). The equivalent spring stiffness was calculated by using the elastic intensity (EI, i.e., bending stiffness) of the track girder and was compared with the spring stiffness of the measured track girder. The comparison showed that the difference between the measurement and analysis was less than approximately 6%, whereas the two results almost matched at the center.

The equivalent spring stiffness of the track girder obtained from the analysis and measurement and the spring stiffness of the rail pad were substituted into Equation (2) to calculate the spring stiffness at the rail supporting points. By using the spring stiffness of the rail supporting points, the TSS was calculated and compared with the measured TSS, as shown in Figure 6(d). As a result, the analytical TSS based on the equivalent spring stiffness calculated by incorporating the bending stiffness of the track girder was very similar to the measured TSS (Figure 6(a)). Therefore, the actual TSS of the direct-fixation-type track system was experimentally and analytically demonstrated to be appropriate when it is evaluated by considering the spring stiffness of the rail pad and the equivalent spring stiffness considering the bending stiffness of the track girder, which serves as the rail support.

Table 3: Equivalent spring stiffness for each location on the track girder.

Position	x (m)	EI (N/mm^2)	$k_{\text{track girder}}$ (kN/mm)
Quarter ($L/4$)	2.972	1.05807×10^{15}	196.58
Center ($L/2$)	5.945	3.69337×10^{15}	17.58

Note. x = distance from the track girder support bearing; L = 11.890 m (span length of the track girder, supporting distance); EI = the bending stiffness of the track girder; $k_{\text{track girder}}$ = the equivalent stiffness of the track girder.

4. Conclusions

In this study, numerical analyses and field measurements were conducted to analyze the TSS that reflects the structural characteristics of the DFT on the YGB. The results are as follows:

(1) The DFT on the YGB is supported by a track girder that is relatively flexible. Therefore, the TSS of the DFT is directly influenced by the stiffness, namely, the deflection, of the track girder. Thus, the actual TSS of the DFT could be evaluated as the TSS, which is combined with the spring stiffness of the rail pad and the equivalent spring stiffness, which is substituted from the bending stiffness of the track girder of the rail support.

(2) Moreover, the actual TSS of the DFT system supported by the track girder was determined through both a numerical analysis and field measurements. Therefore, the results can be applied as the input data for a simulation to predict the performance of the DFT system in the future. Furthermore, the actual TSS of the DFT on the YGB can be useful when evaluating the performance of existing DFTs and the maintenance of the tracks.

(3) As a result, the TSS of the DFT was directly installed at the upper girder that should be considered for the bending stiffness of the girder. Also, the TSS of the DFT should practically evaluate the behavior of the track girder structure.

Data Availability

The data used to support the findings of this study are available from the corresponding author upon request.

Conflicts of Interest

The authors declare that they have no conflicts of interest.

Acknowledgments

The present study was conducted with funding from the Airport Railroad Co., Ltd. (Research on evaluation of track component damage and maintenance plan for direct fixation track of Yeongjong Grand Bridge, unpublished data, 2015). The authors wish to express their sincere appreciation to all those who were involved in this study.

References

[1] G. Gu and J. Choi, "The dynamic response of rail support," *Vehicle System Dynamics*, vol. 51, no. 6, pp. 798–820, 2013.

[2] D. Martino, "*Train-bridge interaction on freight railway lines*," M.S. thesis, KTH Architecture, Stockholm, Sweden, 2011.

[3] P. Lou, Z.-W. Yu, and F. T. K. Au, "Rail-bridge coupling element of unequal lengths for analysing train-track-bridge interaction systems," *Applied Mathematical Modelling*, vol. 36, no. 4, pp. 1395–1414, 2012.

[4] V. N. Dinh, K. D. Kim, and P. Warnitchai, "Dynamic analysis of three-dimensional bridge-high-speed train interactions using a wheel-rail contact model," *Engineering Structures*, vol. 31, no. 12, pp. 3090–3106, 2009.

[5] B. Biondi, G. Muscolino, and A. Sofi, "A substructure approach for the dynamic analysis of train-track-bridge system," *Computers and Structures*, vol. 83, no. 28–30, pp. 2271–2281, 2005.

[6] J. A. Zakeri, H. Xia, and J. J. Fan, "Dynamic responses of train-track system to single rail irregularity," *Latin American Journal of Solids and Structures*, vol. 6, no. 2009, pp. 89–104, 2009.

[7] J. Y. Choi, J. S. Chung, J. H. Kim, K. Y. Lee, and S. G. Lee, "Evaluation of behavior of direct fixation track and track girder

ends on Yeongjong Grand Bridge," *Journal of the Korean Society of Safety*, vol. 31, no. 6, pp. 45–51, 2016.

[8] J. Choi, "Influence of track support stiffness of ballasted track on dynamic wheel-rail forces," *Journal of Transportation Engineering*, vol. 139, no. 7, pp. 709–718, 2013.

[9] T. Dahlberg, "Railway track settlements—a literature review, Division of Solid Mechanics," Report for the EU project SUPERTRACK. IKP, Linköping University, Linköping, Sweden, December 2013, http://www-classes.usc.edu/engr/ce/599/Thesis/RTRSETTL.pdf.

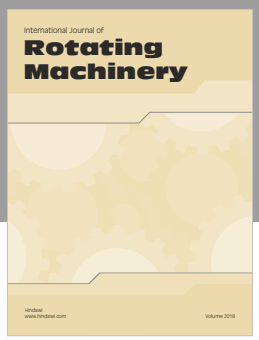

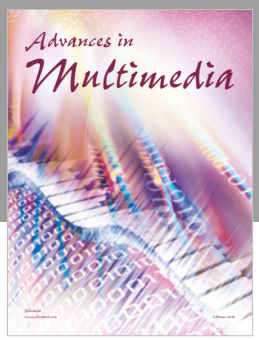

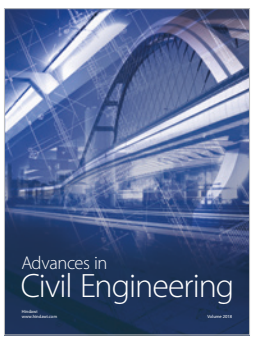

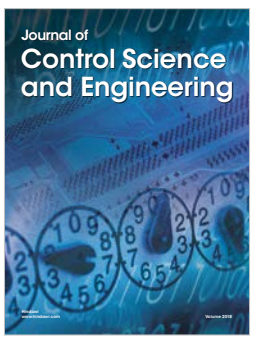

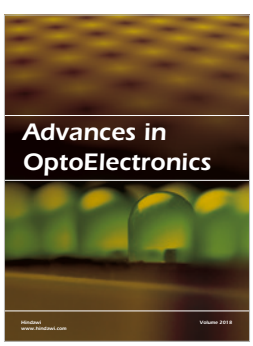

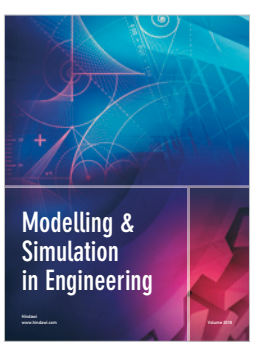

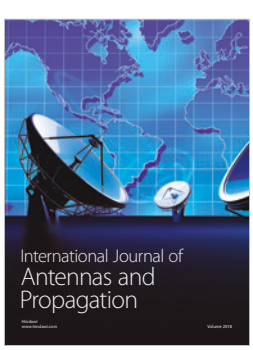

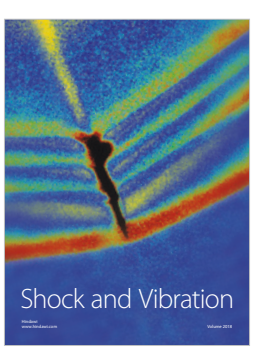

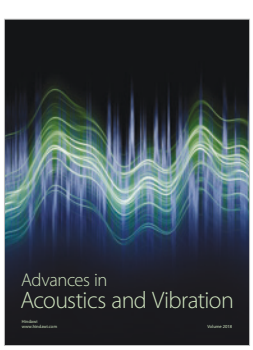

Hindawi

Submit your manuscripts at
www.hindawi.com